Analysis on the characteristics of animal tissues based on the Terahertz time domain spectroscopy system

Chengzhen Lu (卢承振)[1], Chen Liu (刘 晨)[1], Erliang Cui (崔二亮)[1], Jia Li (李 佳)[1], Wei Liu (刘 维)[1*], and Ping Sun (孙 萍)[2]

[1]*Key Laboratory of Terahertz Optoelectronics, Ministry of Education, Department of Physics, Capital Normal University, Beijing 100048, China*

[2]*Beijing Normal University, Beijing Area Major Laboratory of Applied Optics, Department of Physics, Beijing 100875, China*

[*]*Corresponding author: lwei263@263.net*

Received August 17, 2011; accepted October 27, 2011; posted online April 18, 2012

THz spectral properties of several of fresh animal tissues are investigated based on the time domain system. Terahertz pulse transmission spectra of different animal tissues slices with different thickness are obtained, and the refractive index, the absorption coefficient, and the extinction coefficient of these tissues are analyzed and discussed. According to the double Debye model, tissue parameters are simulated and calculated. The theoretical and experimental results are matched. These studies are helpful to make further research of the THz spectral performances of human tissues and cancers.

OCIS codes: 320.7100, 320.7150.
doi: 10.3788/COL201210.S13201.

The terahertz spectroscopy has the advantages of non-ionization and low average power, thus it is not thought to be hazardous to the tissues of human. Furthermore, the terahertz waves can excite the vibration mode and rotation mode of macromolecules. Both amplitude and phase information of materials which are detected and then contrasted can be gotten. Compared with visible light and infrared, it also has the advantage of low scattering, so the surface character and depth pattern of samples can be acquired at the same time. Therefore, it makes the terahertz detection in the field of biomedicine possible to measure the tissue in vivo without any damage.

In recent years, with the development of the technology of the terahertz radiation source and detection source, the technology of terahertz imaging is developing rapidly. Intermolecular transition models can be detected by the terahertz radiation. In addition, the vibration frequency of DNA, RNA, and protein molecules lie in terahertz wave band, and information of these molecules can be detected coherently using terahertz radiation[1,2]. Terahertz imaging can detect skin inflammation, such as dermatitis, eczema, and psoriasis, etc. It is reported that human tissues can be imaged *in vivo* and *vitro* by the technology of terahertz radiation and distinguish diseased[3,4], normal and inflamed tissue in quality[4−6]. THz-CT imaging has the spatial resolution of sub-millimeter, and it is possible to replace X-CT with THz-CT imaging[2]. In 2004 and 2006, various cancer types and organs were studied by Fitzgerald *et al*, which means that THz imaging can be used to give the tumor margins in fresh tissues[7−9]. However, terahertz imaging can analyze the difference between tumour tissues and normal tissues in quality at present.

In this letter, in order to distinguish normal tissues, inflammation and tumor tissues, different kinds of slices with different thickness are tested and analyzed based on THz-TDS (terahertz time domain spectrometer) system in transmission geometry. The refractive index, the extinction coefficient, and the absorption coefficient of tissues are obtained to provide the proof of experiments and theories for distinguishing different tissues in quantification.

Based on the Z-3 THz-TDS system working in transmission geometry, the block diagram of elements is shown in Fig. 1, in which the mode-locked Mai-Tai laser generates femtosecond pulse with 800 nm center wavelength, pulse width less than 120 fs and pulse power 1 W. The mechanism of THz beam emission is that femtosecond laser illuminates InAs wafer to produce the photoinduced Dember electric field with the carrier accelerated by additional bias voltage. The Terahertz detection mechanism is linear electro-optic Pockels effect. A polarizer, quarter wave plate and a Wollaston Prism separate the light into two orthogonal polarized lights. Then the change in polarization is detected by the balanced photodiodes. The delay line with the 200 Hz sawtooth oscillating scans the entire THz pulse in order to obtain the THz field as a

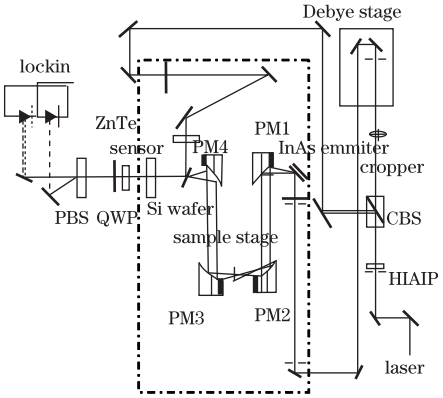

Fig. 1. Block diagram of THz elements.

function of delay and amplitude.

The THz-TDS works at room temperature (about 298 K), which is put into a box purged full with nitrogen gas to keep the relative humidity less than 4% and enhance the SNR. During experiments, the THz beam is focused on the quartz–N_2 interface at an incident angle of 90°, and THz beam path is N_2-quartz-tissue-quartz-N_2. Before the experiment, an empty sampling cell is tested as a contrast to get rid of the changes of signal from quartz, and then THz beam path is N_2-quartz-vacuum-quartz-N_2.

Data processing methods of the experiment are based on the physical models of acquiring the THz optics parameters of materials[10]. And the refractive index $n_s(\omega)$, the absorption coefficient $\alpha_s(\omega)$ and the extinction coefficient $K_s(\omega)$ with the change of frequency are calculated by the formulas as follows

$$n_s(\omega) = \phi(\omega)c/\omega d + 1, \quad (1)$$

where $\phi(\omega)$ is the phase difference between the sample and the reference signal, c is the velocity of light in vacuum, d is the thickness of the sample, and ω is the angular frequency of terahertz.

The extinction coefficient and the absorption coefficient meet the following equations:

$$K_s(\omega) = \frac{c}{\omega d}\ln[n_s(\omega)(n_q+1)^2/\rho(\omega)(n_q+n_s(\omega))^2], \quad (2)$$

$$\alpha_s(\omega) = 2K_s(\omega)\omega/c = 2\ln[n_s(\omega)(n_q+1)^2/\rho(\omega)(n_q+n_s(\omega))^2]/d, \quad (3)$$

where n_q is the refractive index of quartz, $\rho(\omega)$ is the modulus ratio of the amplitude between the sample and the reference.

According to the Eqs. (1) and (3), the refractive index and absorption coefficient are worked out by OriginPro7.5. The refractive indexes of pork adipose, chicken, beef, and pork kidney with the thicknesses of 40 and 50 μm, respectively in the range from 0.2 THz to 2.5 THz are shown in Fig. 2. It can be seen that the refractive index decreases basically in near line with the increase of frequency. Thus, the refractive index presents abnormal dispersion[11] from 0.2 THz to 1.5 THz which is considered as effective spectrum range.

The absorption coefficient from 0.2 to 2.5 THz is shown in Fig. 3. And there is a trend of increasing in line from 2.1 to 2.3 THz in Fig. 3(a). The refractive index and absorption coefficient of another three tissues have the similar results, however, the parameters values of different tissues are different in the same frequency condition.

According to the experimental results, relative parameters are given in Table 1. It can be found that refractive indexes of different tissues are different at 0.51 and 0.99 THz. As to the same tissue, such as beef, refractive indexes have no clear distinction between the thicknesses of 40 and 50 μm, which is considered to be equal. The same results can be gotten for the chicken with the thickness of 40 and 50 μm, which shows that thickness of tissues have no influence on refraction index.

But the absorptive coefficient increases with the increase of thickness. However, the result of chicken has some problem. The reason is that chicken tissue is not

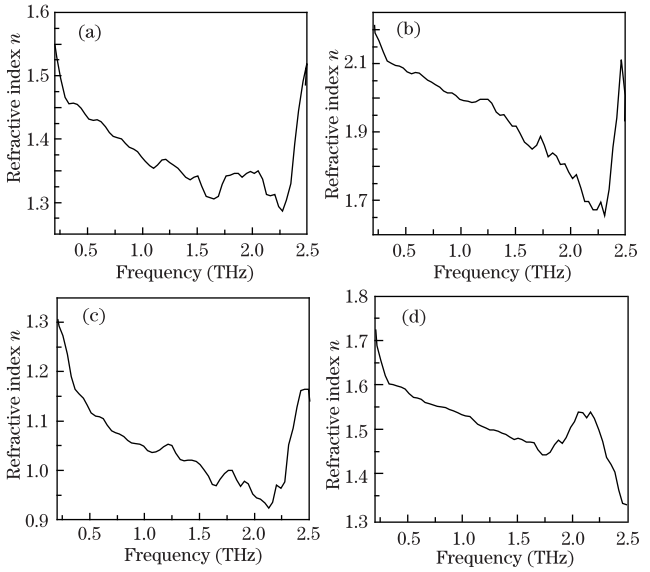

Fig. 2. Refractive indexes of (a) pork adipose, (b) beef, (c) chicken, and (d) pork kidney with the thicknesses of 40 and 50 μm from 0.2 to 2.5 THz.

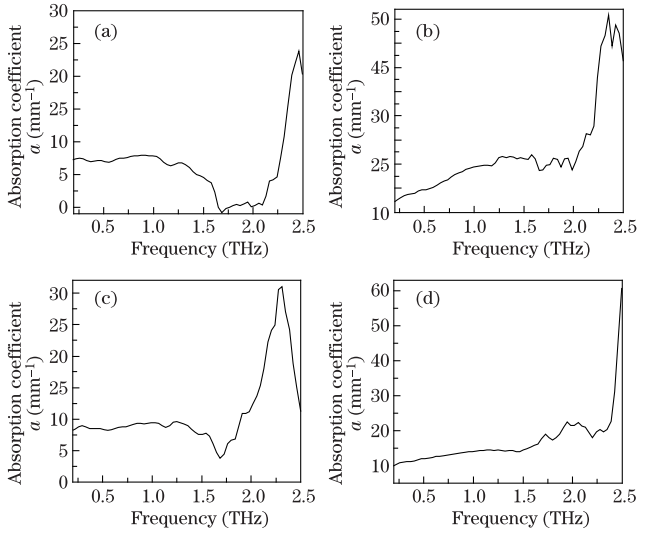

Fig. 3. Absorption coefficients of (a) pork adipose, (b) beef, (c) chicken, and (d) pork kidney with the thicknesses of 40 and 50 μm from 0.2 to 2.5 THz.

Table 1. Refractive Index (n), Absorption Coefficient (a) of Different Tissues

	n	n	a (mm^{-1})	a (mm^{-1})
	0.51 THz	0.99 THz	0.51 THz	0.99 THz
Pork Adipose	1.43132	1.372664	6.96183	7.86950
Beef Broken 40	2.07203	1.99976	13.6616	15.4756
Beef 50	2.07677	1.99673	14.7163	19.3892
Pork Liver 30	3.05086	2.99872	12.8572	13.9067
Pork Liver 50	0.217886	0.147343	–	–
Pork Kideny 50	1.58058	1.53283	12.0198	13.9079
Pork Kideny 30	0.40947	0.420095	–	–
Chicken 50	1.11677	1.048654	8.32280	9.40068
Chicken 40	1.16291	1.073524	8.57131	8.99913

compacter than beef tissue, which can result in computational deviation. Then absorptive coefficient gradient of beef is obtained with the value 10.547 mm^{-1} at 0.51 THz and 39.136 mm^{-1} at 0.99 THz. The refractive index of pork kidney with the thickness of 50 μm is lower and has a greater deviation because of much thinner tissue, whose main reason is that the phase delay becomes smaller and the influence of noise in the experimental system cannot be ignored. Pork liver with the thickness of 50 μm presents the same result. For the ultra-thin samples, only when there is very high stability of the system, the material parameters can be gotten correctly by THz-TDS system.

It can be concluded from above results that tissue parameters can be used as an experimental evidence to distinguish different tissues quantitatively, such as the parameters of beef and adipose above.

Because of a lot of water in the bio-tissue, water accords with a double Debye model with a slow relaxation mode τ_1 and a fast relaxation mode τ_2[12]. Hence, it is reasonable to simulate bio-tissues with the double Debye mode approximately. The complex dielectric constant and frequency of the double Debye mode meets the function as follows:

$$\widetilde{\varepsilon}(\omega) = \varepsilon_\infty + \frac{\varepsilon_\mathrm{s} - \varepsilon_2}{1+\omega^2\tau_1^2} + \frac{\varepsilon_2 - \varepsilon_\infty}{1+\omega^2\tau_2^2} - \mathrm{i}\left(\frac{\omega\tau_1(\varepsilon_\mathrm{s} - \varepsilon_2)}{1+\omega^2\tau_1^2} + \frac{\omega\tau_2(\varepsilon_2 - \varepsilon_\infty)}{1+\omega^2\tau_2^2}\right), \quad (4)$$

where ε_s is the static dielectric constant, ε_∞ is the limiting value at high frequency, and ε_2 is the value at an intermediate frequency. Considering $\widetilde{\varepsilon}(\omega) = \varepsilon'(\omega) - \mathrm{i}\varepsilon''(\omega)$ and getting the following equations:

$$\varepsilon' = [n(\omega)]^2 - [k(\omega)]^2, \quad (5)$$

$$\varepsilon'' = 2n(\omega)k(\omega). \quad (6)$$

From Eqs. (5) and (6), the variation curve of the real part and imaginary part of dielectric constant with frequency can be gotten. The dielectric curve of beef with the thickness of 50 μm is shown in Fig. 4, in which the real part of the curve from 0.2 to 1.5 THz is given in Fig. 4(a), and the imaginary part of the curve is shown in Fig. 4(b). The real part curve of beef fitted by double Debye model from 0.2 to 1.5 THz is depicted in Fig. 5(a), according to Eq. (4), while the imaginary part curve is shown in Fig. 5(b), in which the solid line stands for the simulated double Debye curve. The correlation coefficient is 0.95 in Fig. 5(a) and 0.66 in Fig. 5(b). The approximate double Debye parameters of beef tissues are first obtained as shown in Table 2.

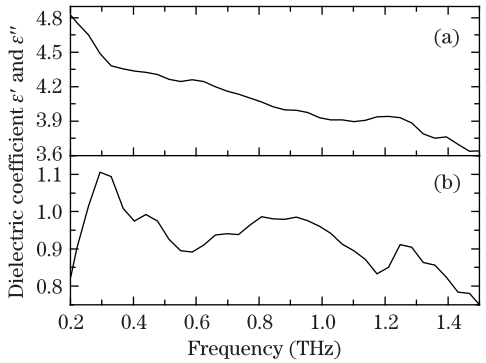

Fig. 4. Dielectric constant curve of beef with the thickness of 50 μm at different frequencies are extracted from the full frequency spectrum. (a) The curve of the real part of dielectric constant; (b) the curve of the imaginary part of dielectric constant in the range from 0.2 to 1.5 THz.

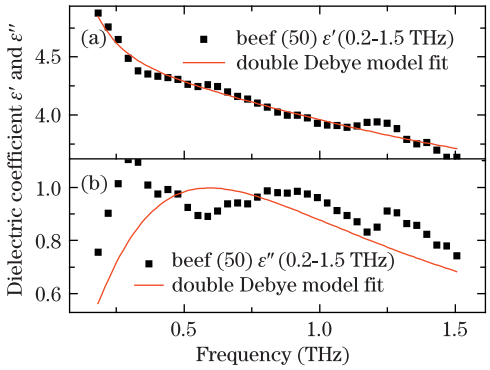

Fig. 5. Dielectric constant curve fitted by double Debye model. (a) The curve of the real part of dielectric constant; (b) the curve of the imaginary part of dielectric constant in the range from 0.2 to 1.5 THz.

Table 2. Fitted Parameters of Double Debye Model for the Beef

	ε_s	ε_2	ε_∞	τ_1 (s)	τ_2 (s)
Value	6.35902	4.32055	3.12899	8.99704	0.69307

Dielectric constant of animal tissue can be got by the THz-TDS technology and double Debye mode, and as basic physical parameters, it is of great significance in theory and practice for further study electric field-dielectric interaction. Different animal tissues have different Debye coefficients. They can be looked as the experiment standard for distinguishing tissues. What's more, ε_s, ε_∞, ε_2, τ_1, and τ_2 can be gotten without the limit of frequency, so it has more theoretical meaning and useful value to distinguish different tissues in quantity.

In conclusion, the spectrum characteristics of different animal tissues with different thickness are tested and analyzed, and refractive indexes, absorption coefficients of several animal tissues at 0.51 and 0.99 THz are gotten. Thickness has basically no effect on the refractive index of bio-tissues, and absorption increases with the increase of thickness. Different animal tissues have different refractive indexes in the THz regime, so different animal tissues can be distinguished quantitatively in the experiment. In addition, the double Debye model of beef is given, and the approximate parameters of beef tissue are obtained based on its dielectric constant curve with the change of frequency. This work has potentially practical value in distinguishing among cancer tissues, diseased tissues, and normal tissues in quantification.

This work was supported by the Beijing Natural Science Foundation of China (No. 4102031) and the Beijing Educational Committee Science and Technology Project (No. KM200810028007).

References

1. F. Zhang and X. Feng, Chin. Comput. Med. Mag (in Chinese) **12,** 429 (2006).
2. L. Sun, G. Wang, and J. Zhang, Appl. Opt. (in Chinese) **26,** 4 (2005).
3. E. Pickwell, B. E. Cole, A. J. Fitzgerald, M. Pepper, and V. P. Wallace, Phys. Med. Biol. **49,** 1595 (2004).
4. M.-A Brun, F. Formanek, A. Yasuda, M. Sekine, N. Ando, and Y. Eishii, Phys. Med. Biol. **55,** 4615 (2010).
5. M. W. Ruth, E. C. Bryan, P. W. Vincent, J. P. Richard, D. A. Donald, H. L. Edmund, and P. J. Michael, Phys. Med. Biol. **47,** 3853 (2002).
6. R. M. Woodward, V. P. Wallace, D. D. Arnone, E. H. L Linfield, and M. Pepper, J. Biol. Phys. **29,** 257 (2003).
7. P. W. Vincent, F. T. Philip, J. F. Anthony, M. W. Ruth, C. Julian, J. P. Richard, and D. A. Donald, Faraday Discussions **126,** 255 (2004).
8. P. W. Vincent. J. F. Anthony, P. Emma, J. P. Richard, F. T. Philip, F. Niamh, and H. Thomas, Appl. Spectrosc. **60,** 1127 (2006).
9. J. F. Anthony, P. W. Vincent, B. Lynda, J. P. Richard, D. P. Anand, and D. A. Donald, Radiology **239,** 533 (2006).
10. X. Wang and W. Wang, Acta Clinical Sonica (in Chinese) **20,** 2248 (2008).
11. Y. Li, Y. Zheng, and W. Wang, Journal of Capital Normal University (Natural Science Edition) (in Chinese) **3,** 28 (2007).
12. E. Pickwell and V. P. Wallace, J. Phys. D: Appl. Phys. R **39,** 301 (2006).